Polymer-Plastics Technology and Engineering**,** Volume 58, Issue 16, 2019, pp. 1757-1765

DOI: 10.1080/25740881.2019.1576194

# Non Isothermal cure kinetics of Aerogel/Epoxy composites using Differential Scanning Calorimetry

Suryanarayanan Krishnaswamy[1*], Veronica Marchante[1], Hrushikesh Abhyankar[1], Zhaorong Huang[2], James Brighton[1]

[1]Advanced Vehicle Engineering Centre- Cranfield University, UK, [2]Surface Engineering & Precision Institute- Cranfield University, UK

**Corresponding Author:**
Suryanarayanan Krishnaswamy
School of Aerospace, Transport and Manufacturing, Cranfield University
Email: s.krishnaswamy@cranfield.ac.uk

**Abstract:** The present work determines the non-isothermal cure parameters of aerogel/epoxy samples along with the effect of a wetting agent. The cure parameters were calculated using Kissinger and isoconversional methods after which the reaction was modelled with the Sestak-Berggren equation. It is seen that the composites had higher activation energy and frequency factor values compared to the pure resin and, similarities in cure parameters between the aerogel/epoxy composites with and without the wetting agent were seen. Hence the former's use is advocated due to its positive influence on the resin-aerogel interface without sacrificing the cure parameters.

**Keywords:** Aerogel, Epoxy, Cure Kinetics, DSC, Activation Energy

## 1 Introduction

Aerogels are materials with highly porous structures, large specific surface areas, low densities and excellent thermal insulation properties [1, 2] prepared by replacing the liquid in a gel with air [3]. Typically, the thermal conductivity values of silica aerogel are between 0.01 to 0.03 W/(m K) [4] thereby resulting in numerous applications as thermal insulators. Hrubesh [5] and Schmidt & Schwertfeger [6] in their respective studies have detailed various applications of aerogels including uses as insulators in, amongst others, cryogenics, space vehicles, portable coolers and transport vehicles. Although the numerous small pores of the aerogel ensures excellent thermal, optical, acoustic and physical properties, the same structure limits the mechanical strength of the material [7] such as their fragility and brittleness [8, 9, 10].To overcome this drawback, a polymer binder is considered and the studies of Wei et al. [10] and Meador et al. [11] show that the introduction of a polymer within the aerogel improves the mechanical properties of the system. Another method of aerogel-epoxy synthesis is the impregnation of the aerogel in a polymer matrix; according to Schmidt & Schwertfeger [6] these binding systems can be divided into wet and dry systems. When comparing the coefficient of thermal resistance, it is seen that a liquid binding system (using dispersion) shows a better performance in comparison to a thermoplastic bound aerogel composite [6]. Hence an epoxy resin system was chosen as a binding material in the present work because of the polymer's wide use in composite materials [12].

The study of cure kinetics and the relationship between the degree of cure and the properties are essential parameters needed to identify optimum cure conditions [13, 14]. When considering the cure kinetics of epoxy resins, Gonis et al. [15] noted that the amount of heat released during cure was indirectly proportional to the number of ethylene oxide units in the epoxy resin. Roşu et al. [16] calculated the activation energy of two different epoxy resins, diglycidyl ether of bisphenol A (DGEBA) and diglycidyl ether of hydroquinone (DGEHQ) using the

isoconversional method and found the activation energy remains independent of the working conditions and almost constant between conversion intervals of 0.3 and 0.6. The curing of epoxy resins is a complex multistep process that could include numerous chemical reactions or a reaction that could have complex effects like vitrification and viscous relaxation [17]. These effects, according to Yoo et al. [18], play a role in decreasing the activation energy towards the end of the cure. The work of El-Taher et al. [19] compared the activation energies and frequency factors for DGEBA resins cured with hydrolysed materials from salt solution and curing agents without salt and, found the values for the former to be higher than the latter. However, the activation energies calculated for the curing agent without the salt solution was similar for the three methods used in the paper (Kissinger, isoconversional and autocatalytic methods) but varied when the material from the salt solution was used.

Montserrat and Malek [14] compared the results of non-isothermal and isothermal data and stated that both methods produce similar results when the curing is primarily controlled by the chemical reaction. However at lower temperature, the authors argue that the problem is more challenging due to effects such as vitrification. When considering the different non-isothermal methods, Hong and Lee [20] calculated the activation energy of silicone rubber using the Kissinger, Ozawa, Flynn-Wall-Ozawa and Friedman methods wherein the methods showed similar results with Friedman method having the lowest value. El-Thaher et al. [19], state that the Kissinger method is more accurate than the Ozawa method for $n^{th}$ order reactions.

The current work considers the effect of aerogel on the cure kinetics of the epoxy resin by studying the cure parameters of a pure epoxy resin and a composite material consisting of aerogel and epoxy. Additionally, the effect of a wetting agent is also explored to assess the suitability of using it in the production of the said composite. The cure parameters, for the reasons discussed above, will be identified using the Kissinger and isoconversional (that

would give the cure parameters as the cure progresses) methods. Then the materials' cure kinetics would be modelled using an autocatalytic equation and validated against experimental data. The results of the three methods are then discussed and compared with each other.

## 2 Materials and Methods

### 2.1 Materials

The aerogel used was the Enova Aerogel IC3110 (Cabot Corporation, USA) which are particles between 100-700μm in size. RS-M135 (PRF composites, UK) was used as the epoxy resin along with a hardener which was a custom blend of RS-MH137 and RS-MH134 (both by PRF composites) in a 2:1 weight ratio wherein both hardeners are amine based systems. The resin and the hardener were then mixed in a 10:3 weight ratio for all samples. Additionally, a wetting agent- BYK-P 9920 (BYK-Chemie, Germany) was used to prepare one of the batches; the wetting agent is a combination of organically modified polydimethylsiloxane, a branched polyolefin and an epoxyfunctional reactive thinner (oral communication from a company representative- April, 2017). The wetting agent was recommended by the company for the above-mentioned materials and the amount used in the present study i.e., 3% (by weight) is the maximum recommended level suggested by the company in the product's data sheet [21].

The first batch of the sample was made from pure epoxy resin and hardener wherein the resin and the hardener were mixed in the required ratio before testing. For the second batch, which included the aerogel, the resin and the hardener were mixed together as previously discussed and then 0.03 (mass fraction) of aerogel was added, mixed and the samples tested. Finally, to prepare the third batch, after the resin was weighed, 3% (by weight) liquid wetting agent was added to the resin using a dropper. The hardener was then introduced and the solution mixed

together before 0.03 (mass fraction) of aerogel was added and the samples tested. It must be noted that the mixing for all the samples were carried out manually.

### 2.2 Differential Scanning Calorimetry

To calculate the cure kinetics, the samples were tested in a Q200 DSC (differential scanning calorimetry (TA instruments, USA) under a 50 mL/min nitrogen purge using the TA Refrigerated Cooling System 90 (RCS 90). The obtained peaks were then analysed using the TA Universal Analysis 2000 (version 4.5A) software.

Each batch was subjected to four dynamic runs at constant heat rates- $5^0$C/min, $10^0$C/min, $15^0$C/min and $20^0$C/min from $40^0$C to $300^0$C. The samples were tested in Tzero Aluminium pans wherein the lids were pressed onto the pans using a sample encapsulation press. It must be noted that efforts were made to maintain the mass of the material in the Tzero pans between 13-16 mg.

The cure kinetic parameters for the three batches were calculated using three different methods and the results compared.

## 3 Results

### 3.1 Dynamic Runs

Figure 1 shows the dynamic DSC curves for the samples in the present study. The samples show an exothermic reaction between ~$50^0$C and ~$250^0$C across all the considered heating rates due to the cure of the resin. Although, individual samples show varying peak heights for different heating rates, the difference between them is small enough to be neglected. Hence, it is believed that the three samples studied have identical behaviour within the heating rates considered.

## 3.2 Kissinger Energy

This method, described by Kissinger [22], calculates the activation energy and the frequency factor from the peak temperatures ($T_p$) using Equation 1.

$$\frac{\boldsymbol{E_{ak}}}{\mathbf{R}} = \frac{\mathbf{d}\left(\ln\frac{\emptyset}{\mathbf{T_p}^{\mathbf{2}}}\right)}{\mathbf{d}\left(\frac{\mathbf{1}}{\mathbf{T_p}}\right)}$$

Equation 1

Where $E_{ak}$ is the activation energy, R is the universal gas constant, ø is the heating rate and $T_p$ is the temperature at the peak.

The activation energies and the frequency factors for the three batches are calculated using Equation 2 and Equation 3 respectively as described in the work of Nordeng [23]. The slope and intercept values are obtained from the Kissinger plots (as shown in Figure 2 for batch 3) for the three batches. The curve was fitted using a linear function ('poly1' model name in MATLAB R2015b) and the $r^2$ values for the three batches are shown in Table 1 wherein, all the values are >0.95.

$$\mathrm{E_{ak}} = -(\mathrm{Slope} \times \mathrm{R})$$

Equation 2

$$\mathrm{A} = ((\mathrm{e}^{\mathrm{Intercept}} \times E_{ak})/\mathrm{R})$$

Equation 3

## 3.3 Isoconversional Method

Although the Kissinger method results in a simple calculation of the activation energy and frequency factor using the peak temperatures, it doesn't give further information on the reaction progress. The isoconversion method, on the other hand, allows the calculation of the

frequency factors and activation energies at different conversion rates, thereby providing additional information on the reaction kinetics [19].

The degree of conversion/cure (α) is calculated according to the formula in [17] whose simplified version is shown in Equation 4.

$$\alpha = \frac{Q(t)}{Q_T}$$

Equation 4

Where $Q_T$ is the total enthalpy (heat) of the reaction and Q(t) is the cumulative heat of the reaction.

$Q_T$ was calculated using the Integrate Peak function and Q(t) was calculated using the Running Integral function, both in the Universal Analysis software. It must also be noted that both values had identical starting and ending points (as shown in Figure 3). The degree of cure (α) as a function of temperature with different heating rates for batch 3 is given in Figure 4 where the temperature at a certain degree of cure is seen to increase with the heating rate.

To calculate the activation energy and the frequency factor using the isoconversion method, Equation 5 is followed [17].

$$\frac{d\left(ln\frac{d\alpha}{dt}\right)}{dT^{-1}} = -\frac{E_{ai}}{R}$$

Equation 5

The values of dα/dt were calculated from α and t and, smoothened using the moving average filter in MATLAB before postprocessing. An example of such a signal before and after smoothening is shown in Figure 5 for the 10°C/min run of batch 3.

Using the smoothened signal, plots for Equation 5 were generated; an example of such a plot is given in Figure 6 for batch 3. The activation energy and the frequency factors are once again calculated using Equation 2 and Equation 3 respectively. The activation energies and frequency factors calculated at various α values for the three batches are tabulated in Table **2** and

Table **3** respectively. For both quantities, the values between 0.3>α>0.7 are shown thereby eliminating the inaccuracies due to peak tails which lead to higher error magnitudes [14]. It must be noted that the $r^2$ values for all the fits were above 0.98.

### 3.4 Autocatalytic Method

In terms of modelling, epoxy resins are usually described by either reaction order kinetics or autocatalytic cure [16, 17]. However, the curing of epoxy always converts the oxygen in the epoxy ring into a hydroxyl group, which in turn, is also a curing group for the epoxy; thereby showing evidence for an autocatalytic model [19]. Therefore, the two parameter Sestak-Berggren equation (representing an autocatalytic model) was chosen to model the cure kinetics of the materials in the present study. The equation, introduced by Sestak & Berggren [24], is shown in Equation 6

$$\frac{d\alpha}{dt} = k\alpha^m(1-\alpha)^n$$

Equation 6

To identify *n* and *m* for each batch, the method outlined in [19, 25, 26] was utilised wherein, the GRG Nonlinear solver in Microsoft Excel 2010 was used to maximise the correlation of the plot between $\ln((d\alpha/dt))/((\alpha^m)*((1-\alpha)^n))$ vs 1000/T by changing the values of *n* and *m*. The values for the 4 heating rates and conversion factors between 0.3≤α≤0.7 for an individual batch were populated in a single plot to deduce the coefficients (as shown in Figure 7). The slope was used to calculate the activation energy (Equation 2) and $\ln(A_{sb})$ was the y-intercept. The values of n, m, activation energies and pre –exponential factors are shown in Table 4.

The absolute value of $r^2$ (Pearson's correlation coefficient) in the table is the value of the maximising objective function whose maximum value was set to 1.

The model was simulated using Equation 7 where the values for $A_{sb}$, $E_{asb}$, $m$ and $n$ are obtained from Table 4 for each batch.

$$\frac{d\alpha}{dt} = A_{sb}\{e^{-E_{asb}/RT} * \alpha^m[(1-\alpha)^n]\}$$

Equation 7

The results are shown and compared with the experimental data for batches 1, 2 and 3 in Figure 8, Figure 9 and Figure 10 respectively. For the sake of clarity, the smoothened dα/dt values were used as the experimental data. Although a good fit between the model and experiment is observed, there is some deviation at higher temperatures (representing higher α values). This is due to the selection of α between 0.3 and 0.7 for the model parameterisation as discussed in the previous section. Nevertheless, it is believed that the truncated Sestak-Berggren model [24] using the parameters identified in Table 4 can adequately model the cure kinetics of the materials in the present study especially, in the mid cure range.

## 4 Discussion

Table **5** shows the activation energies and the frequency/pre-exponential factors determined by the various methods used in the present study. It must be noted that the value used for the isoconversional method for each batch was the average in the interval $0.3 \leq \alpha \leq 0.7$ and the frequency factors for the Sestak-Berggren model were calculated using Equation 3. When comparing the individual results for each method, it is seen that the activation energy of batch 1 (pure resin) is consistently lower than batches 2 and 3 which contain aerogel. This could be explained by the lower viscosity of pure resin that has a lower activation energy [19]. Arabli

and Aghili [27] observed a catalytic effect of silica nanoparticles during the cure of epoxy resin when silica nanoparticles were added (which resulted in a lower activation energy). However in the present study, this effect is not seen because it is believed that the larger aerogel particles (100-700μm) resulted in a more viscous material and inhibited the cross-linking reaction more than the smaller silica nanoparticles used in [27] (average diameter of 12nm); thereby negating the catalytic effect and increasing the activation energies in batches 2 and 3. When comparing the results of batch 2 with batch 3, the activation energy determined by the isoconversional method and the Sestak-Berggren model are similar. The Kissinger method, on the other hand, shows a much greater difference particularity for batches 1 and 3. This could perhaps be explained by the nature of the Kissinger equation, which only utilised the parameters at the peak of cure rather compared to the other two methods that accounted for more of the cure cycle ($0.3>\alpha>0.7$ in the present case). However, the results from the former methods are preferred since they consider more of the cure reaction as compared to only peak parameters in the Kissinger method resulting in greater accuracy. Finally because the addition of a wetting agent into the aerogel/epoxy composite has a minimal effect on the cure kinetics of the resin, its use is recommended due to its influence on the interface of the aerogel and the resin. It is thought that the wetting agent would increase the strength at the boundary and hence, positively influence the mechanical properties of the composite. A link between the efficiency of fibre/filler wetting and mechanical properties is seen in the study by Ellakwa et al [28] where, a higher flexural strength was observed in Kevlar fibres wetted with a filled bonding agent which, according to the authors, could be the result of improved fibre wetting due to this type of bonding agent.

It is seen that the Sestak-Berggren equation models the experimental data quite accurately and can be used to represent the respective materials in the present study. Once again, there is a difference in the model parameters between the epoxy (batch 1) and the aerogel/epoxy

(batches 2 and 3). However, batches 2 and 3 do not show much deviation from each other thereby reiterating previous statements about similarities in the cure kinetics of both aerogel/epoxy samples. Hence, the use of a wetting agent is advocated for reasons identified previously.

## 5 Conclusion

The present work considered the non-isothermal cure kinetics of an aerogel/epoxy composite with and without a wetting agent. A sample made of pure resin was also subjected to similar analysis to aid the comparison. The activation energy and the pre-exponential factors (frequency factors) of all three materials were determined using the Kissinger and isoconversional methods. The parameters were then used to model the cure of the materials using the Sestak- Berggren equation. The theoretical model showed good agreement with the experiment data. The activation energy and frequency factors from all three methods showed a higher value for the aerogel composites when compared to the pure resin thereby suggesting an increased viscosity in the former. Additionally, the results also showed similarities in the cure kinetic parameters between aerogel/epoxy composites with and without the wetting agent. Therefore, the addition of a wetting agent to increase the wettability of the aerogel and hence, improve the interface between it and the resin system is recommended.

Acknowledgements: The authors would like to thank Dr. Alex Skordos, Dr. David Ayre, Dr. Lawrence Cook and Mr. Jim Hurley for their assistance in the preparation of the samples and technical support.

Additional experimental data can be found at: https://figshare.com/s/3714d82e29c829baa00b

References:

(1) Koravos, J.; Norwood, C.; Pescatore, P.; Pidhurney, J. Aerogel Insulative Coatings:

New Coating Technology Offers Personnel Protection http://www.pcimag.com/articles/98016-aerogel-insulative-coatings (accessed Feb 12, 2016).

(2) Jin, L.; Li, P.; Zhou, H.; Zhang, W.; Zhou, G.; Wang, C. Improving Thermal Insulation of TC4 Using YSZ-Based Coating and SiO2 Aerogel. *Prog. Nat. Sci. Mater. Int.* **2015**, *25* (2), 141–146.

(3) Kistler, S. S. Coherent Expanded Aerogels and Jellies. *Nature* **1931**, *127* (3211), 741.

(4) Yuan, B.; Ding, S.; Wang, D.; Wang, G.; Li, H. Heat Insulation Properties of Silica Aerogel/Glass Fiber Composites Fabricated by Press Forming. *Mater. Lett.* **2012**, *75*, 204–206.

(5) Hrubesh, L. W. Aerogel Applications. *J. Non. Cryst. Solids* **1998**, *225*, 335–342.

(6) Schmidt, M.; Schwertfeger, F. Applications for Silica Aerogel Products. *J. Non. Cryst. Solids* **1998**, *225*, 364–368.

(7) Baetens, R.; Petter Jelle, B.; Gustavsen, A. Aerogel Insulation for Building Applications: A State-of-the-Art Review. *Energy Build.* **2011**, *43* (4), 761–769.

(8) Kim, H. M.; Kim, H. S.; Kim, S. Y.; Youn, J. R. Silica Aerogel/Epoxy Composites with Preserved Aerogel Pores and Low Thermal Conductivity. *e-Polymers* **2015**, *15* (2).

(9) Kim, G. S.; Hyun, S. H. Effect of Mixing on Thermal and Mechanical Properties of Aerogel-PVB Composites. *J. Mater. Sci.* **2003**, *38* (9), 1961–1966.

(10) Wei, T.-Y.; Lu, S.-Y.; Chang, Y.-C. Transparent, Hydrophobic Composite Aerogels with High Mechanical Strength and Low High-Temperature Thermal Conductivities. *J. Phys. Chem. B* **2008**, *112* (38), 11881–11886.

(11) Meador, M. A. B.; Fabrizio, E. F.; Ilhan, F.; Dass, A.; Zhang, G.; Vassilaras, P.; Johnston, J. C.; Leventis, N. Cross-Linking Amine-Modified Silica Aerogels with Epoxies: Mechanically Strong Lightweight Porous Materials. *Chem. Mater.* **2005**, *17* (5), 1085–1098.

(12) Ivankovic, M.; Brnardic, I.; Ivankovic, H.; Mencer, H. J. DSC Study of the Cure Kinetics during Nanocomposite Formation: Epoxy/Poly(Oxypropylene) Diamine/Organically Modified Montmorillonite System. *J. Appl. Polym. Sci.* **2006**, *99*, 550–557.

(13) Hayaty, M.; Beheshty, M. H.; Esfandeh, M. Isothermal Differential Scanning Calorimetry Study of a Glass/Epoxy Prepreg. *Polym. Adv. Technol.* **2011**, *22* (6), 1001–1006.

(14) Montserrat, S.; Malek, J. A Kinetic Analysis of the Curing Reaction of an Epoxy Resin. *Thermochim. Acta* **1993**, *228* (C), 47–60.

(15) Gonis, J.; Simon, G. P.; Cook, W. D. Cure Properties of Epoxies with Varying Chain Length as Studied by DSC. *J. Appl. Polym. Sci.* **1999**, *72* (11), 1479–1488.

(16) Roçu, D.; Caçcaval, C. N.; Mustaça, F.; Ciobanu, C. Cure Kinetics of Epoxy Resins Studied by Non Isothermal DSC Data. *Thermochim. Acta* **2002**, *383*, 119–127.

(17) Sbirrazzuoli, N.; Vyazovkin, S. Learning about Epoxy Cure Mechanisms from Isoconversional Analysis of DSC Data. *Thermochim. Acta* **2002**, *388* (1–2), 289–298.

(18) Yoo, M. J.; Kim, S. H.; Park, S. D.; Lee, W. S.; Sun, J. W.; Choi, J. H.; Nahm, S. Investigation of Curing Kinetics of Various Cycloaliphatic Epoxy Resins Using Dynamic Thermal Analysis. *Eur. Polym. J.* **2010**, *46* (5), 1158–1162.

(19) El-Thaher, N.; Mekonnen, T.; Mussone, P.; Bressler, D.; Choi, P. Nonisothermal DSC

Study of Epoxy Resins Cured with Hydrolyzed Specified Risk Material. *Ind. Eng. Chem. Res.* **2013**, *52* (24), 8189–8199.

(20) Hong, I.-K.; Lee, S. Cure Kinetics and Modeling the Reaction of Silicone Rubber. *J. Ind. Eng. Chem.* **2013**, *19* (1), 42–47.

(21) BYK Chemie. BYK-P 9920 https://www.byk.com/en/additives/additives-by-name/byk-p-9920.php.

(22) Kissinger, H. E. Reaction Kinetics in Differential Thermal Analysis. *Anal. Chem.* **1957**, *29* (11), 1702–1706.

(23) Nordeng, S. H. Determination of Activation Energy and Frequency Factor for Samples of the Bakken Formation ( Miss . – Dev .): Williston Basin , ND. *North Dakota Geol. Surv.* **2012**, No. 163, 1–15.

(24) Šesták, J.; Berggren, G. Study of the Kinetics of the Mechanism of Solid-State Reactions at Increasing Temperatures. *Thermochim. Acta* **1971**, *3* (1), 1–12.

(25) Pérez-Maqueda, L. A.; Criado, J. M.; Sánchez-Jiménez, P. E. Combined Kinetic Analysis of Solid-State Reactions: A Powerful Tool for the Simultaneous Determination of Kinetic Parameters and the Kinetic Model without Previous Assumptions on the Reaction Mechanism. *J. Phys. Chem. A* **2006**, *110* (45), 12456–12462.

(26) Vyazovkin, S.; Burnham, A. K.; Criado, J. M.; Pérez-Maqueda, L. A.; Popescu, C.; Sbirrazzuoli, N. ICTAC Kinetics Committee Recommendations for Performing Kinetic Computations on Thermal Analysis Data. *Thermochim. Acta* **2011**, *520* (1–2), 1–19.

(27) Arabli, V.; Aghili, A. The Effect of Silica Nanoparticles, Thermal Stability, and

Modeling of the Curing Kinetics of Epoxy/Silica Nanocomposite. *Adv. Compos. Mater*. **2015**, *24* (6), 561–577.

(28) Ellakwa, A. E.; Shortall, A. C.; Marquis, P. M. Influence of Fiber Type and Wetting Agent on the Flexural Properties of an Indirect Fiber Reinforced Composite. *J. Prosthet. Dent.* **2002**, *88* (5), 485–490.

**List of Tables:**

Table 1 Peak model parameters

| Batch | Rate (°C/min) | Peak Temperature (°C) | Kissinger Parameters | | |
|---|---|---|---|---|---|
| | | | $r^2$ | Activation Energy ($E_{ak}$) (kJ/mol) | $\ln(A_k)$ |
| Pure Resin (Batch 1) | 5 | 100.95 | 0.9921 | 41.49 | 11.59 |
| | 10 | 121.08 | | | |
| | 15 | 130.41 | | | |
| | 20 | 137.57 | | | |
| Resin + Aerogel (Batch 2) | 5 | 104.19 | 0.9997 | 60.03 | 17.77 |
| | 10 | 116.98 | | | |
| | 15 | 125.08 | | | |
| | 20 | 130.42 | | | |
| Resin + Wetting Agent + Aerogel (Batch 3) | 5 | 104.65 | 0.9542 | 51.05 | 14.82 |
| | 10 | 113.76 | | | |
| | 15 | 127.67 | | | |
| | 20 | 134.44 | | | |

Table 2 Isoconversion activation energies at various values of α

| Conversion | Activation Energies ($E_{ai}$) (kJ/mol) | | |
|---|---|---|---|
| | Batch 1 | Batch 2 | Batch 3 |
| 0.3 | 50.33 | 58.67 | 54.93 |
| 0.4 | 52.65 | 58.90 | 58.32 |
| 0.5 | 54.07 | 58.28 | 59.56 |
| 0.6 | 53.25 | 58.65 | 61.97 |
| 0.7 | 54.08 | 61.27 | 62.99 |
| **Mean** | **52.87** | **59.15** | **59.55** |

Table 3 Isoconversion frequency factors at various values of α

| Conversion | Frequency factors ($\ln(A_i)$) | | |
|---|---|---|---|
| | Batch 1 | Batch 2 | Batch 3 |
| 0.3 | 22.48 | 25.45 | 24.14 |
| 0.4 | 23.06 | 25.28 | 25.01 |
| 0.5 | 23.23 | 24.76 | 25.08 |
| 0.6 | 22.56 | 24.43 | 25.39 |
| 0.7 | 22.27 | 24.63 | 25.06 |
| **Mean** | **22.72** | **24.91** | **24.93** |

Table 4 Model Parameters

| Batch | n | m | $E_{asb}$ (kJ/mol) | $\ln(A_{sb})$ ($min^{-1}$) | $r^2$ |
|---|---|---|---|---|---|
| 1 | 1.86 | 0.16 | 53.04 | 15.51 | 0.997 |
| 2 | 1.98 | 0.03 | 59.45 | 17.61 | 0.997 |
| 3 | 1.99 | 0.03 | 59.54 | 17.56 | 0.997 |

Table 5 Comparison of the parameters from the different methods used in the study; 1-Kissinger Method, 2-Isoconversion method, 3- Sestak-Berggren model

| Parameter | Batch 1 | | | Batch 2 | | | Batch 3 | | |
|---|---|---|---|---|---|---|---|---|---|
| | 1 | 2 | 3 | 1 | 2 | 3 | 1 | 2 | 3 |
| Activation Energy ($E_a$) (kJ/mol) | 41.49 | 52.87 | 53.04 | 60.03 | 59.15 | 59.45 | 51.05 | 59.55 | 59.54 |
| Frequency Factor (lnA) | 11.59 | 22.72 | 24.27 | 17.77 | 24.91 | 26.48 | 14.82 | 24.93 | 26.44 |

**List of Figures:**

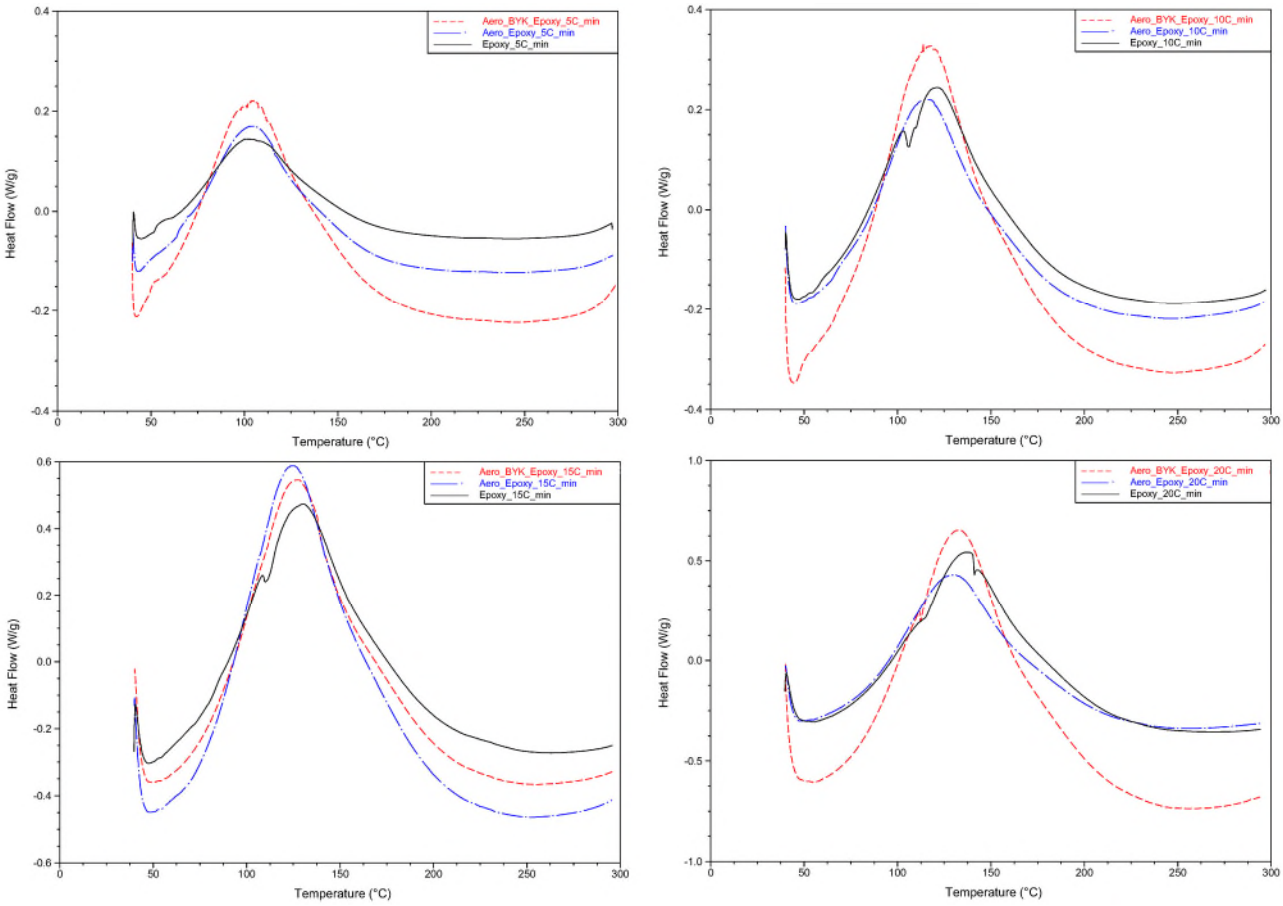


Figure 1 Dynamic runs of the samples in the present study at different heating rates;

(Clockwise from the top) 5°C/min, 10°C/min, 20°C/min and 15°C/min

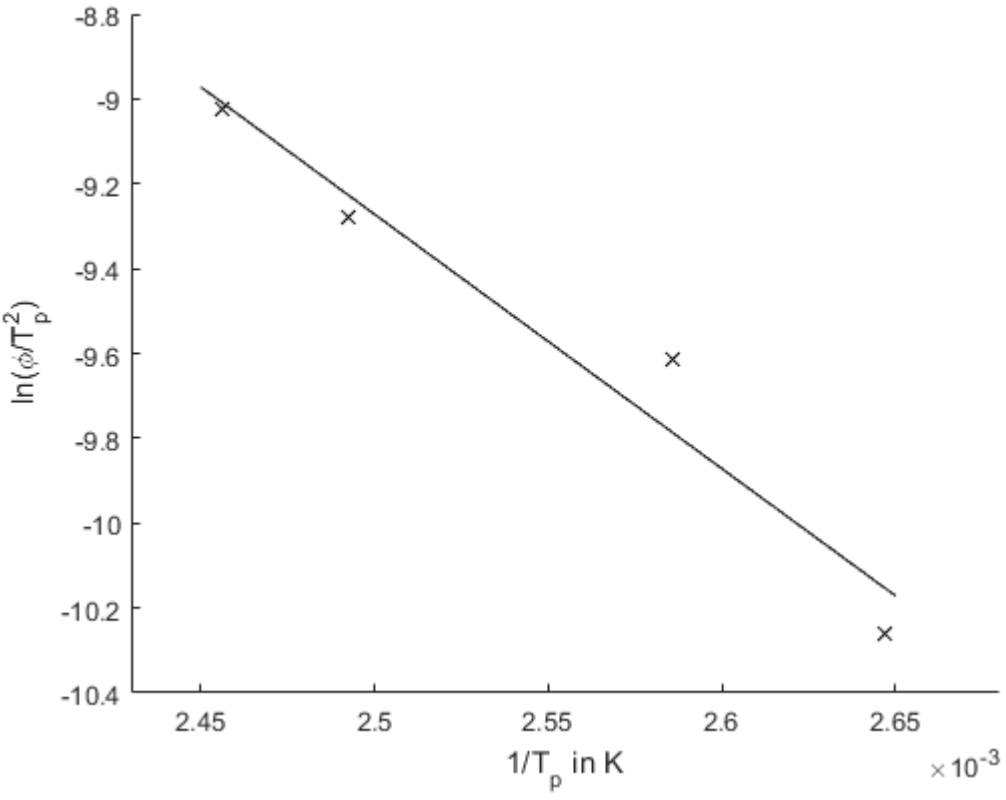


Figure 2 Kissinger plot for Batch 3

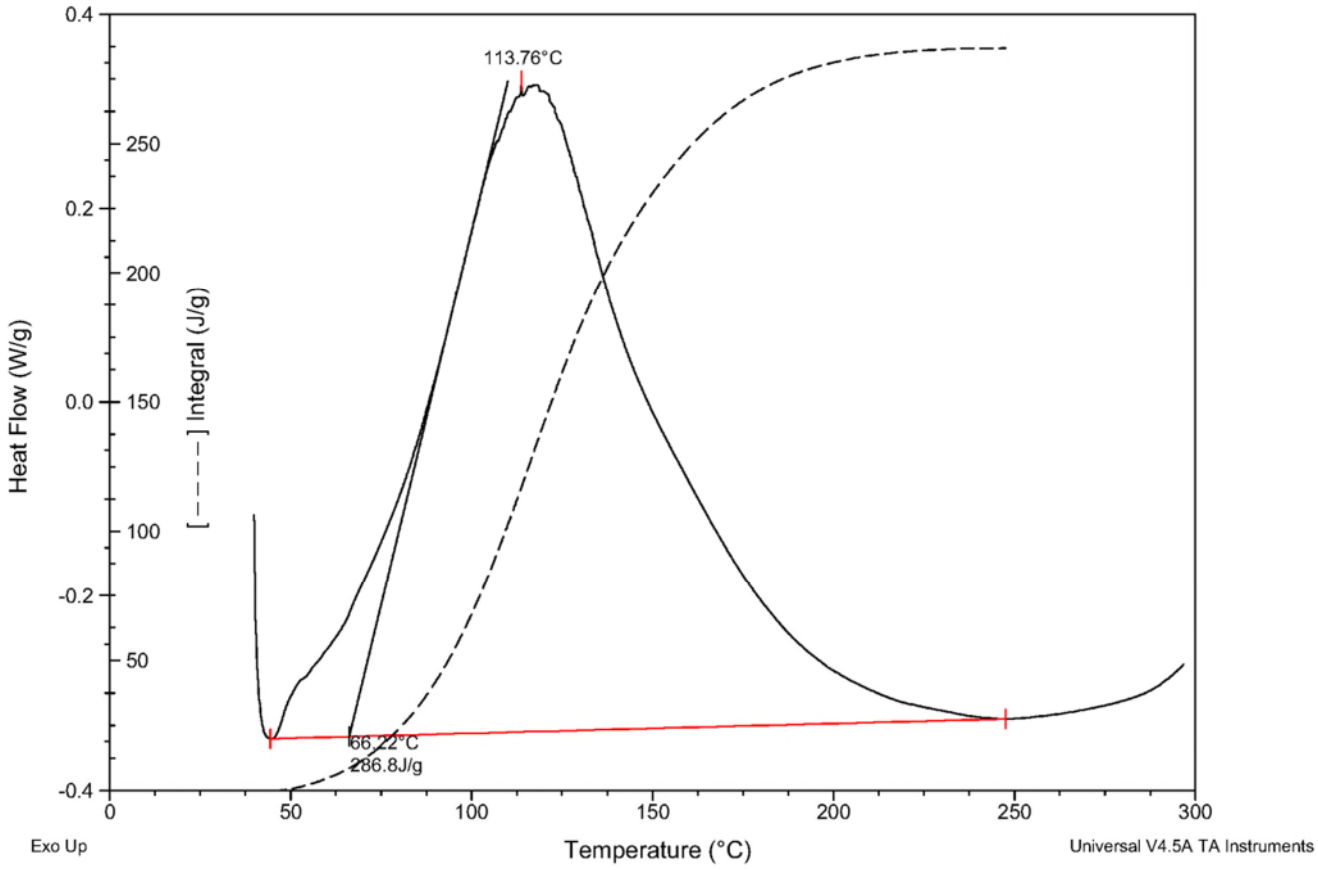


Figure 3 Peak and Running Integral for Batch 3 at $10^0$C/min

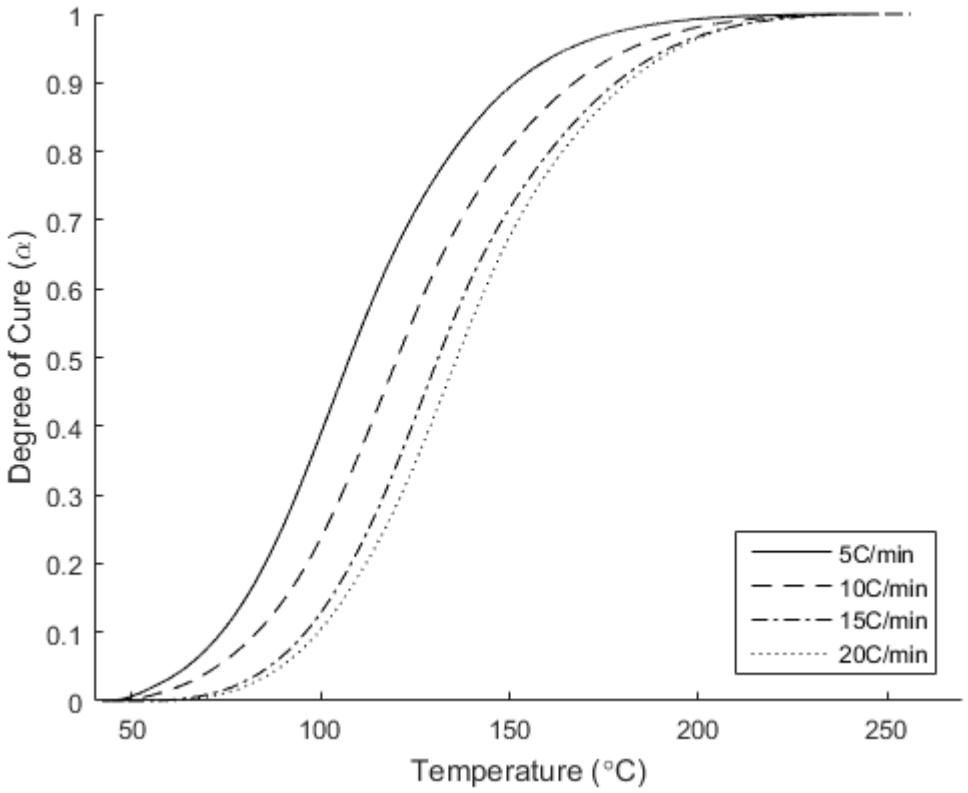


Figure 4 Degree of cure with respect to temperature for different heating rates (Batch 3)

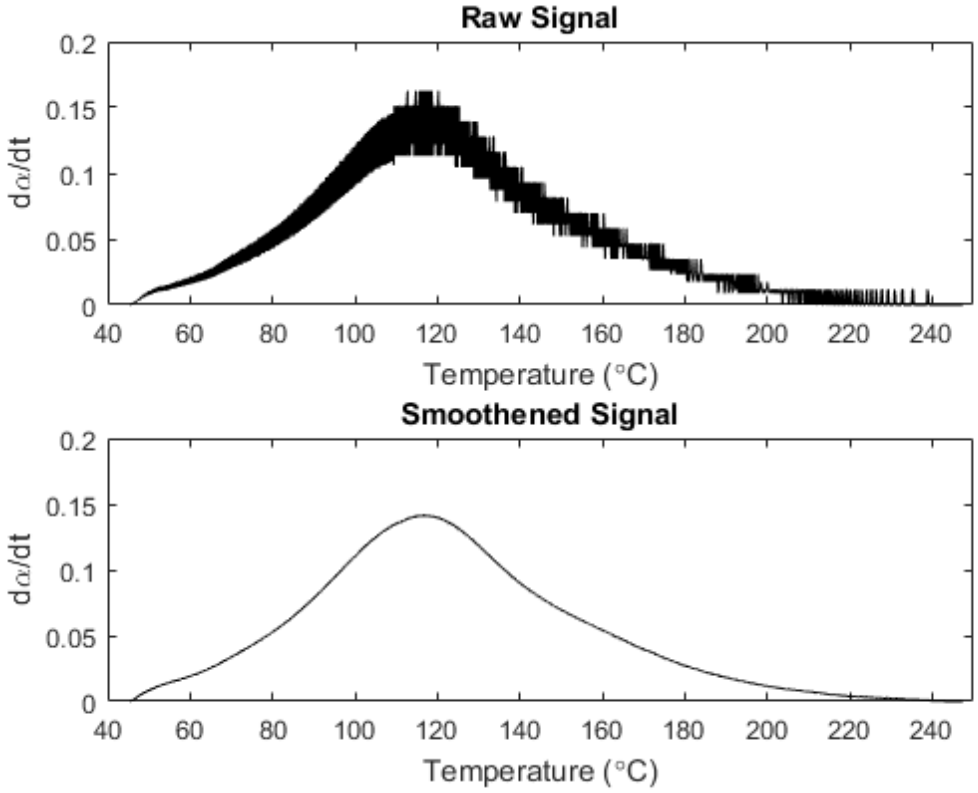


Figure 5 Raw and smoothened signal of dα/dt for batch 3 $10^0$C/min

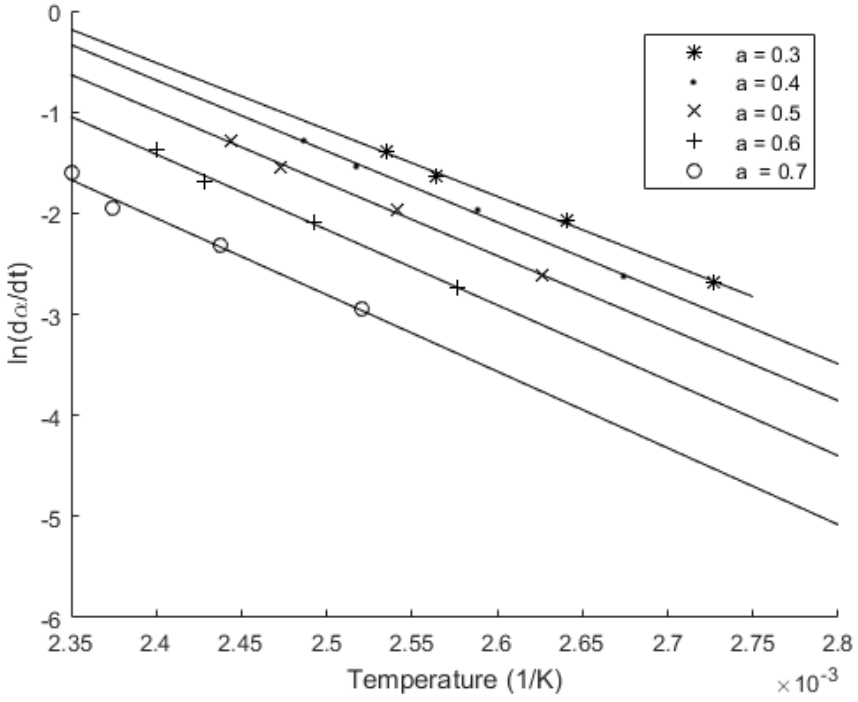


Figure 6 Arrhenius plots for constant degrees of cure (Batch 3)

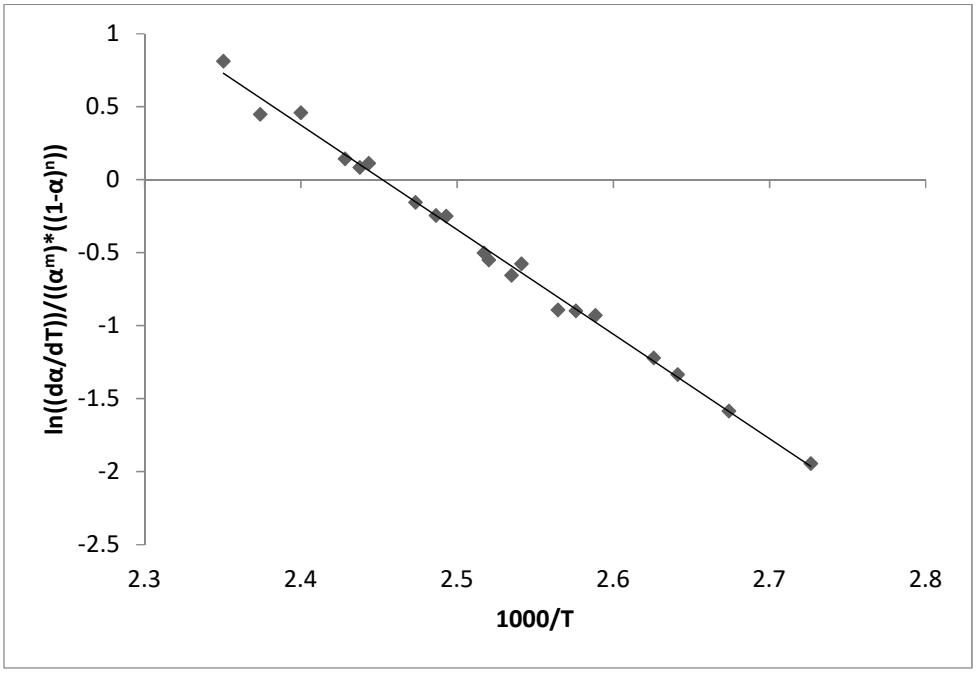


Figure 7 *n* and *m* value calculation for batch 3

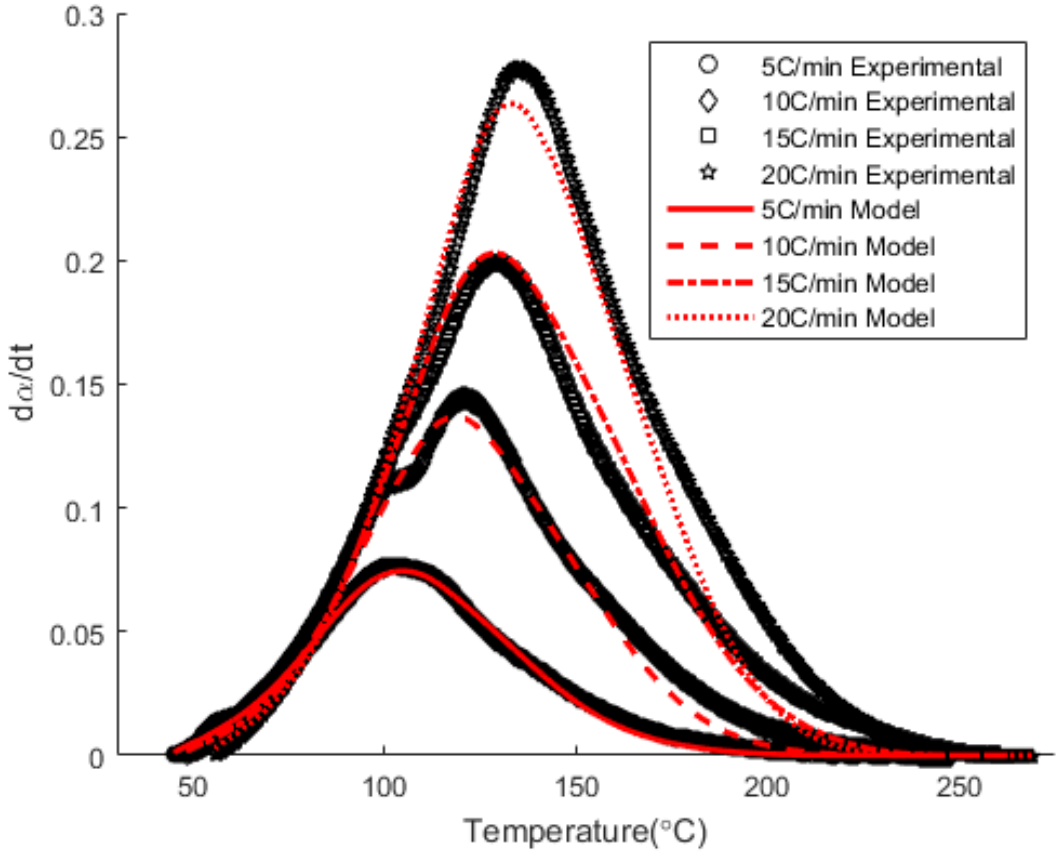


Figure 8 Comparison of model and experimental data for Batch 1

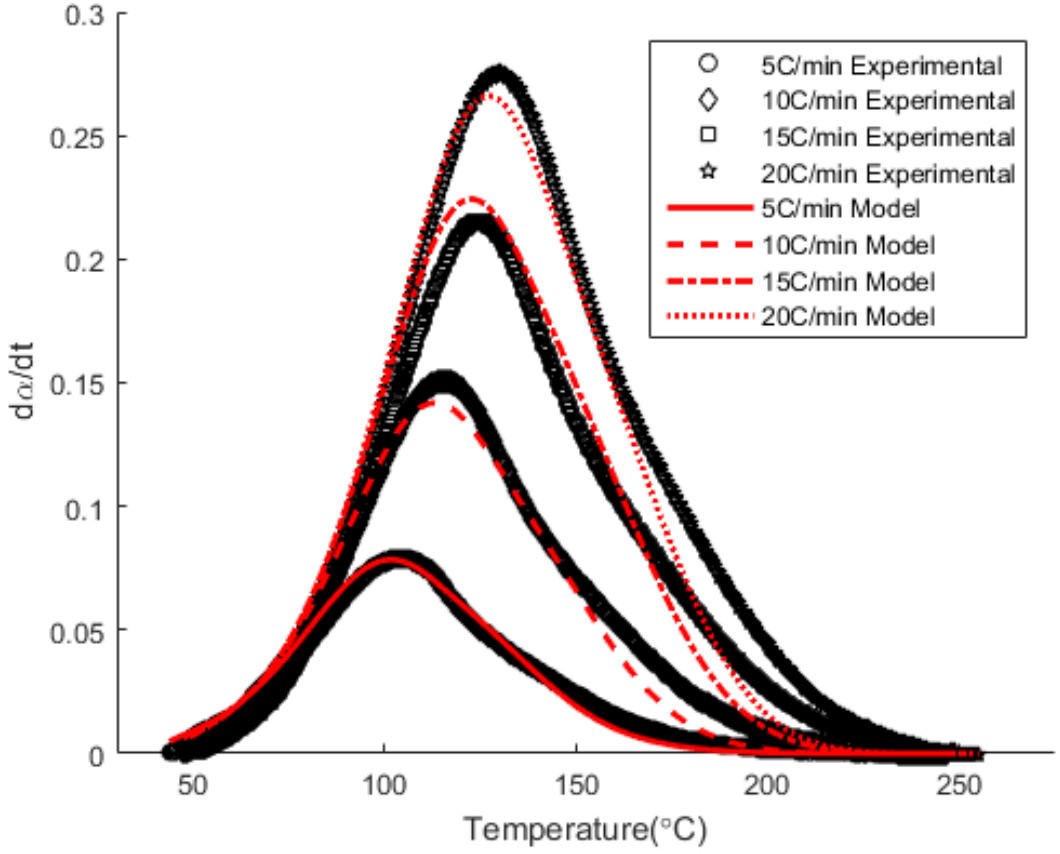


Figure 9 Comparison of model and experimental data for Batch 2

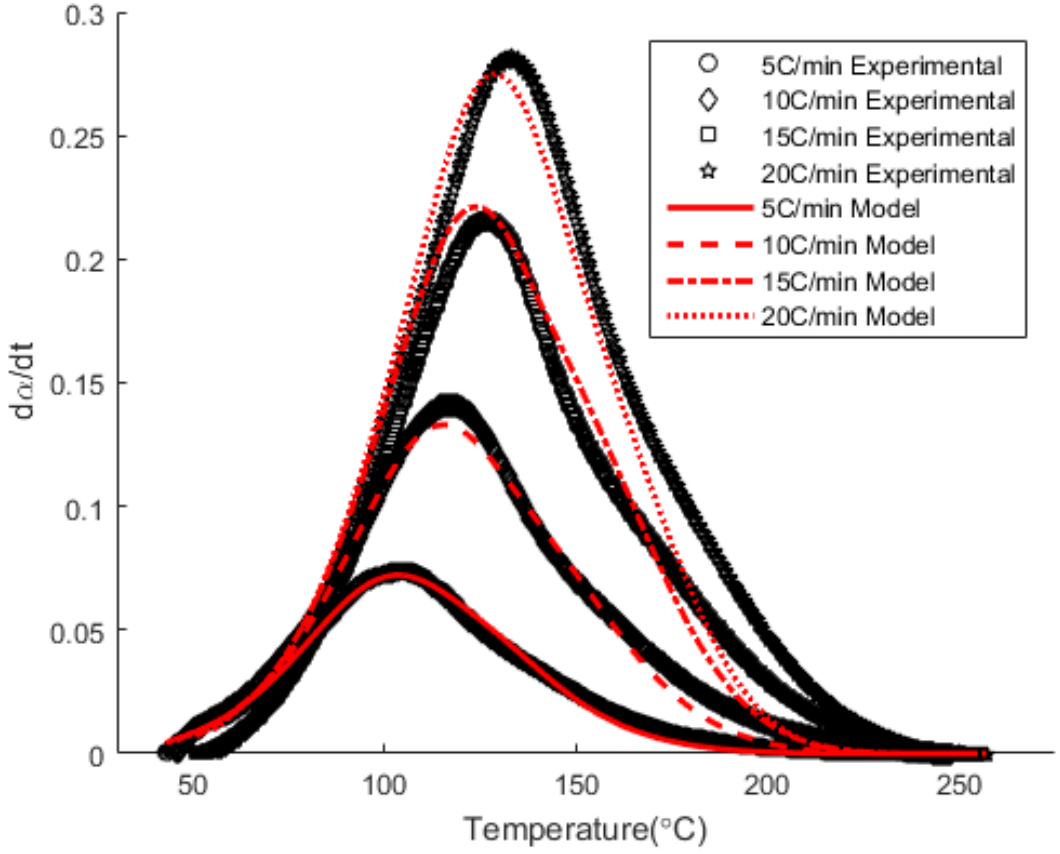


Figure 10 Comparison of model and experimental data for Batch 3